J. agric. Engng Res. (1995) **61,** 73–80

REVIEW PAPER

An Integrated Approach to Soil Compaction Prediction†

A. C. Bailey,* R. L. Raper,* C. E. Johnson,§ and E. C. Burt*

* National Soil Dynamics Laboratory, USDA-ARS, Auburn, AL, 36831-3439, U.S.A.
§ Agricultural Engineering Department, Alabama Agricultural Experiment Station, Auburn University, AL, 36849-5417, U.S.A.

(Received 27 May 1993; accepted in revised form 8 March 1995)

Several areas of study are contributing to the development of procedures to predict soil compaction from machinery traffic. Stresses at the soil–tyre interface are being measured. Analytical and finite element analyses are being used to predict stresses throughout the soil profile. Constitutive stress–strain relationships link soil stresses to compaction and strain. Measured stress states in the soil profile provide intermediate validation of the procedures. This paper summarizes research on measurement of soil–tyre interface stresses, measurement of stress states in the soil profile, the development of soil constitutive relationships and analytical and finite element methods to represent the soil compaction process.

1. Introduction

Soil compaction continues to be a challenge to production agriculture. Excessive soil compaction may diminish crop yields, increase tillage energy consumption, accelerate erosion, and lead to inefficient use of water and nutrients. Additional field operations and energy may be required to remove unwanted soil compaction. The development of procedures that are able to predict the effects of trafficking the soil in a particular state would be a powerful tool for production agriculture. Such procedures would allow farmers to make management decisions based on the trade-off between timeliness and future cost of reclaiming damaged soil structure. Such procedures would also be valuable to engineers as they face the continuing challenge of producing effective and efficient agricultural machines.

Schafer *et al.*[1] presented overall objectives and basic requirements for modelling soil–machine interactions. An undertaking of this scope requires an understanding of several basic phenomena. First, the nature of soil–tyre interface stresses must be understood. Second, the types of stresses occurring within the soil profile must be known. Third, a constitutive stress–strain relationship for agricultural soils is necessary to relate stresses to strains within the profile. Finally, all this information must be integrated into predictive procedures using either analytical or numerical techniques such as the finite element method. This paper is a review of recent research in these areas at the USDA–ARS National Soil Dynamics Laboratory and the Agricultural Engineering Department, Alabama Agricultural Experiment Station, Auburn University, both in Auburn, Alabama, USA.

2. Measurement of soil–tyre interface stresses

Soil movement starts at the soil–tyre interface. Knowledge about the stresses at the soil–tyre interface is crucial to the development of a successful soil compaction prediction procedure because these interface stresses are the inputs to any stress-based procedure that would predict compaction within the soil caused by a tyre. Both the normal and tangential stresses on the tyre surface must be measured because the tangential stresses are an important part of the soil–tyre interaction. In addition to measuring these interface stresses, the distribution and orientation of both stresses are necessary before the stresses can be integrated into horizontal and vertical forces. On a flexible pneumatic tyre this is complicated. The sidewall and lug structure of the tyre can create large variations in the pressure profiles across the surface, so measurements must be made at several locations. Also, the location and orientation of each transducer may not be known once it contacts the soil and the surrounding tyre deflects.

Vanden Berg and Gill[2] measured the normal stress distribution across the width of a smooth tyre. Pressure transducers were embedded either in the tyre or in the soil surface. They found that the shape and

† Alabama Experiment Station Journal No. 2-923225
Presented at Ag Eng 92, Uppsala, Sweden, 1–4 June, 1992

0021-8634/95/060073 + 08 $08.00/0

magnitude of the pressure distribution differed greatly with soil type and condition. Firm soils generated considerably more interface pressure than soft soils. They also found that higher inflation pressures tended to shrink the tyre footprint and increase pressures across the tyre. Decreasing inflation pressure increased the size of the footprint and decreased the pressures. In all cases pressures tended to be higher near the edge of the tyre footprint than at the centre. Trabbic *et al.*[3] found that the maximum values measured between the lugs were approximately 50% of the magnitude of the interface stresses measured on the lugged area. Krick[4] developed a double-membrane transducer that was capable of measuring the normal, tangential and lateral forces on a rigid wheel and flexible rubber tyre. The large size of the transducers, however, prevented them from being used on the surface of the lug.

Burt *et al.*[5] developed a system that measured the magnitudes, locations and directions of interface stresses on an agricultural tyre with lugs. A bi-directional transducer was designed that used a small commertially available pressure sensor mounted on the end of a cantilevered beam (*Fig. 1*). The pressure sensor measured the normal stress and strain gauges on the cantilevered beam measured strain due to the bending moment created by the tangential force on the pressure sensor. This measurement was then converted to a tangential stress at the soil–tyre interface. Three of these transducers were embedded at locations across the lug of a tyre, and two were embedded in the undertread area (area between the lugs). A sonic digitizer installed within the pneumatic tyre measured the location and orientation of each of the five transducers with respect to a known point on the wheel rim (*Fig. 2*). From these measurements the horizontal and vertical components of the interface stress could be calculated and integrated into horizontal (thrust) and vertical forces.

Typical data obtained from one pass of one interface transducer through the soil–tyre contact area are shown in *Fig. 3*. In *Fig. 3* the tyre should be visualized as moving from right to left and rotating counterclockwise. The transducer is directly beneath the wheel axle when the angle is 270 deg, and in front of the wheel axle when the angle is less that 270 deg. An interesting but not completely understood phenomenon is that occasionally the tangential stress measured at the soil–tyre interface is greater than the measured normal stress. This suggests that the traction phenomenon may be more than just simple friction between tyre and soil.

The development of this system for measuring both the direction and magnitude of soil–tyre interface stresses has greatly increased understanding of the loads that are placed on the soil surface by a tyre. These loads are particularly important to any soil compaction procedure because they represent the stress inputs from the real world. This system has been used by Wood and Burt[6] and Wood *et al.*[7] to analyse thrust and motion resistance components of a tractor tyre, and by Burt *et al.*[8] to determine footprint shape and size. The challenge of how to incorporate these data into a soil compaction predictive procedure has not yet been completely solved.

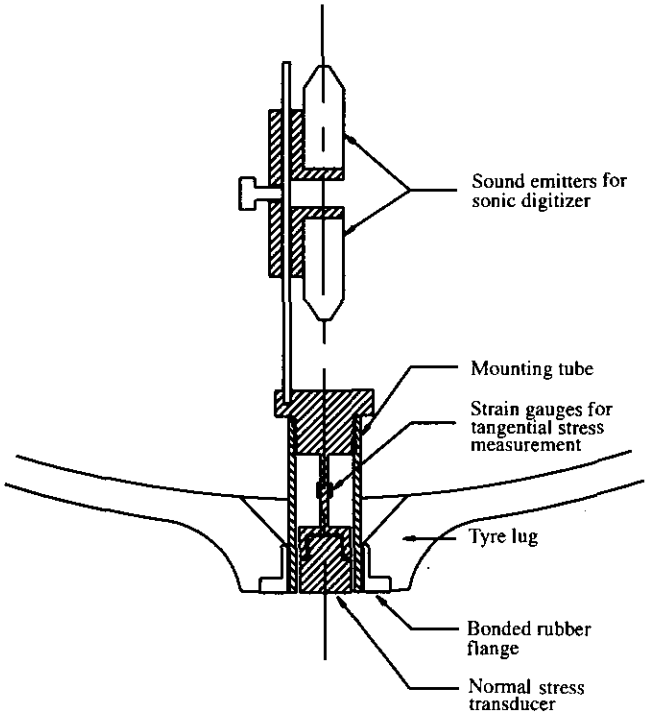

Fig. 1. Transducer for measurement of normal and tangential soil–tyre interface stresses

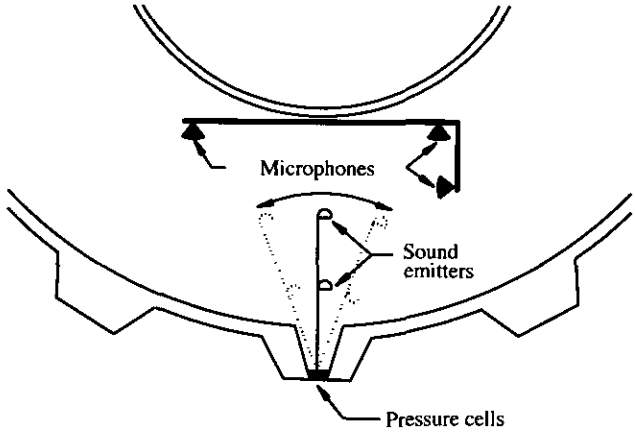

Fig. 2. Position measuring system installed within the air cavity of a pneumatic tyre

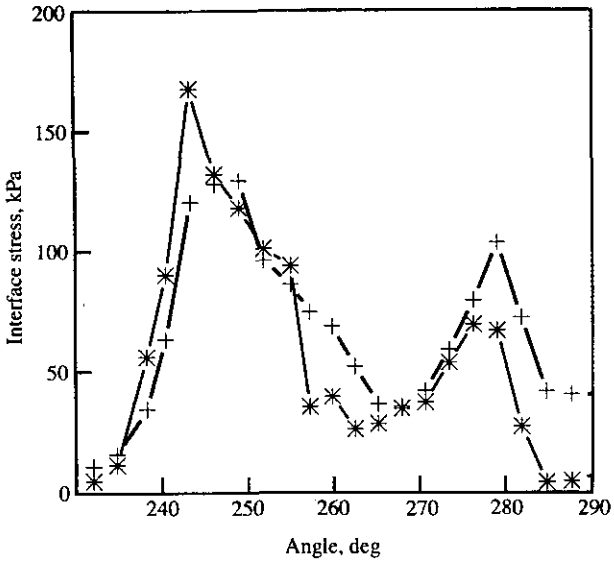

Fig. 3. Typical tangential (+), and normal (*) stresses from a soil–tyre interface transducer. The tyre is rotating counterclockwise. The transducer is directly beneath the axle at 270 degrees and in front of the axle at angles less than 270 degrees

3. Development of a soil stress–strain relationship

3.1. *Stress at a point*

Stress at a point is a 3×3 symmetric matrix or tensor (Malvern[9]) with six independent components often expressed as σ_x, σ_y, σ_z (the normal stresses), τ_{xy}, τ_{xz} and τ_{yz} (the shear stresses). A 3×3 real symmetric matrix has three invariants which define three eigenvalues and eigenvectors. The eigenvalues are the three principal stresses and the eigenvectors define the planes on which the principal stresses act. Thus, the stress state can be expressed in terms of the three principal stresses; σ_1, σ_2 and σ_3 and their directions. A plane that is at equal angles to the three principal stresses is an octahedral plane and the normal and shear stresses that act on this plane are the octahedral normal stress

$$\sigma_{oct} = (\sigma_1 + \sigma_2 + \sigma_3)/3 \tag{1}$$

and the octahedral shear stress

$$\tau_{oct} = \sqrt{(\sigma_1 - \sigma_2)^2 + (\sigma_2 - \sigma_3)^2 + (\sigma_3 - \sigma_1)^2}/3 \tag{2}$$

The octahedral normal stress is also called mean normal stress. The three principal and two octahedral stresses and their directions are independent (invariant) of the orientation of the original three mutually orthogonal planes (x, y and z directions) in the material.

3.2. *A stress–strain relationship for soil*

Stress–strain relationships are the constitutive equations important for prediction of soil compaction and yield. In their classic paper, Vanden Berg *et al.*[10] presented the theoretical background for their hypothesis that soil compaction was probably governed by the mean (octahedral) normal stress. If the soil behaved similarly to a solid continuum, then the stresses should be largest near the application of the load and should decrease downward from this point. However, Söhne *et al.*[11] observed that the maximum amount of soil compaction occurred below the soil surface. Thus, it appeared that continuum theory was not fully applicable to soils.

Bailey and Vanden Berg[12] then proposed a yield diagram for unsaturated soils using mean (octahedral) normal and maximum shear stress. Their yield diagram was based on a three-dimensional yield diagram for saturated soil proposed by Roscoe *et al.*[13] Later, Bailey *et al.*[14] proposed Eqn (3) as a constitutive equation for soil subjected to a hydrostatic stress

$$\bar{\epsilon}_v = (A + B\sigma_h)(1 - e^{-C\sigma_h}) \tag{3}$$

where $\bar{\epsilon}_v$ is the natural volumetric strain; σ_h is the hydrostatic stress; and A, B and C are compactibility coefficients. The hydrostatic stress state is a special stress state in which all principal stresses, σ_1, σ_2 and σ_3, are equal and there are no deviatoric or shear stresses. The hydrostatic stress is the same as the octahedral normal stress, but the term hydrostatic stress was used to emphasize that no shear stresses were present.

Eqn (3) represents the natural volumetric strain of an initially loose, cylindrical soil sample under hydrostatic compression. Bulk density can be obtained from natural volumetric strain by using the relationship

$$\bar{\epsilon}_v = \log_e (V/V_0) = \log_e (\rho_0/\rho) \tag{4}$$

where V, V_0, ρ and ρ_0 are current volume, initial volume, current bulk density and initial bulk density, respectively. Thus, the bulk density can be obtained from Eqn (4) using $\bar{\epsilon}_v$ from Eqn (3)

$$\rho = \rho_0/e^{\bar{\epsilon}_v} \tag{5}$$

More recently, Bailey and Johnson[15] expanded Eqn (3) to represent the cylindrical stress state of the triaxial test

$$\bar{\epsilon}_v = (A + B\sigma_{oct})(1 - e^{-C\sigma_{oct}}) + D(\tau_{oct}/\sigma_{oct}) \tag{6}$$

where σ_{oct} is the octahedral normal stress; τ_{oct} is the octahedral shear stress; and A, B, C and D are compactibility coefficients. The coefficients A, B and C have the same values in both Eqns (3) and (6).

Eqn (6) represents the natural volumetric strain of an initially loose, cylindrical soil sample under a monotonically increasing cylindrical stress state. It does not represent soil reaction to decreasing stress levels. It was developed from modified triaxial tests on several soils using various stress loading paths, but contains the restriction common to triaxial tests that the intermediate and minor principal stresses, σ_2 and σ_3, are equal. An upper boundary of the octahedral shear stress is reached when maximum density (or minimum volume) is attained. When maximum density is attained, the soil undergoes strain at constant volume, a condition that is considered to be plastic flow, and further increases in shear stress will cause no further increase in density. This limit was found to be a linear function of the octahedral normal stress, and may be represented by $\tau_{oct}/\sigma_{oct} \leq K$. This limit on the octahedral shear stress becomes important when using Eqn (6) in finite element analyses.

Coefficients A, B, C and D are determined from triaxial tests. Coefficients A, B and C are determined using non-linear curve fitting techniques using the hydrostatic portion of triaxial data (no shear or deviatoric stress). Coefficient D is determined from the shear stress loading part of triaxial tests. It is most easily determined from tests in which shear loading occurred at constant octahedral normal stress,[15] but can be determined from conventional triaxial tests. Coefficients A, B, C and D have been determined for several soils. These coefficients are unique for each soil and may change with changes in moisture content. Also, the soil must be uniformly prepared for testing because of the small sample size. Despite these limitations, this constitutive relationship provides an accurate determination of soil density at a given stress state in the soil profile. For this reason, Eqns (3) and (6) have been used as the stress–strain relationships for finite element analyses of the soil compaction process.

4. Measurement of soil stresses

Another area of interest in soil compaction research is the measurement of the stress state in the soil profile. This knowledge is critical to the verification of constitutive equations and also serves as an intermediate evaluation of proposed compaction procedures. As discussed in Section 3.1, stress at a point is a 3×3 real symmetric matrix or tensor which may have no more than six unique components. Thus, six stresses are required to define the stress state within a material with respect to any arbitrary x, y, z directions not in the directions of the principal stresses. Measurement of the stress state requires the measurement of six unique stresses from which one can calculate σ_x, σ_y, σ_z, τ_{xy}, τ_{xz} and τ_{yz}. Nichols *et al.*,[16] expanding on concepts proposed by Harris,[17] developed a stress state transducer (SST) that used small commercially available pressure transducers to measure the normal pressure acting on six unique planes (*Fig. 4*). Three of the planes were mutually orthogonal (the planes of p_x, p_y and p_z) and three were non-orthogonal (the planes of p_1, p_2 and p_3) (*Fig. 5*). The directions of the three non-orthogonal planes were chosen to keep all six pressure sensors in close proximity and provide a balanced contribution in the calculation of the shear stresses acting on the x, y and z planes. The direction cosines of the plane of p_1 are all 0·5774 with respect to the x, y and z axes. The direction cosines of the plane of p_2 are −0·5774, 0·5774 and 0·5774 with respect to the x, y and z axes, respectively. The direction cosines of the plane of p_3 are 0·5774, −0·5774 and 0·5774 with respect to the x, y and z axes, respectively. Shear stresses are calculated from the six measured pressures (p_x, p_y, p_z, p_1, p_2 and p_3) from the following equations

$$\begin{aligned} \tau_{xy} &= -0{\cdot}75(p_2 + p_3) + 0{\cdot}5(p_x + p_y + p_z) \\ \tau_{xz} &= 0{\cdot}75(p_1 + p_3) - 0{\cdot}5(p_x + p_y + p_z) \\ \tau_{yz} &= 0{\cdot}75(p_1 + p_2) - 0{\cdot}5(p_x + p_y + p_z) \end{aligned} \tag{7}$$

The three principal stresses and other stresses, such as the normal stress and shear stress on the octahedral plane, can then be calculated.

Typical stresses beneath a tyre calculated from measurements made with a SST beneath the tyre are shown in *Fig. 6*. Stresses at positive distances are in front of the axle. The relative importance of various components of the complete stress state can be seen in the figure. The continued development and use of

Fig. 4. Stress state transducer (SST)

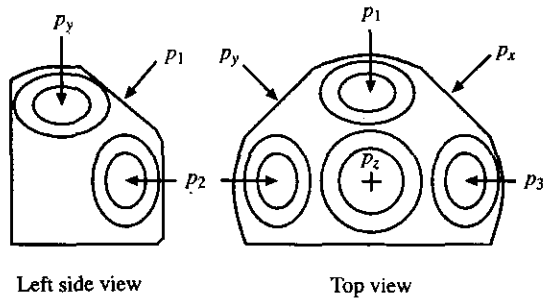

Fig. 5. Stress state transducer (SST)

these transducers will provide data that will help to verify soil compaction prediction procedures as well as expand understanding of how applied stresses are distributed throughout the soil profile.

5. Development of compaction prediction procedures

The next area of interest is the distribution of stresses (or strains) throughout the soil profile. This step involves the integration of all previous information and results in a procedure to predict soil stresses or compaction. Two major approaches have been pursued. One approach combines the Frölich and modified Cerruti equations to provide an "analytical" equation to predict soil stresses. The other approach uses the finite element method to predict the stress and strain distribution within the soil profile.

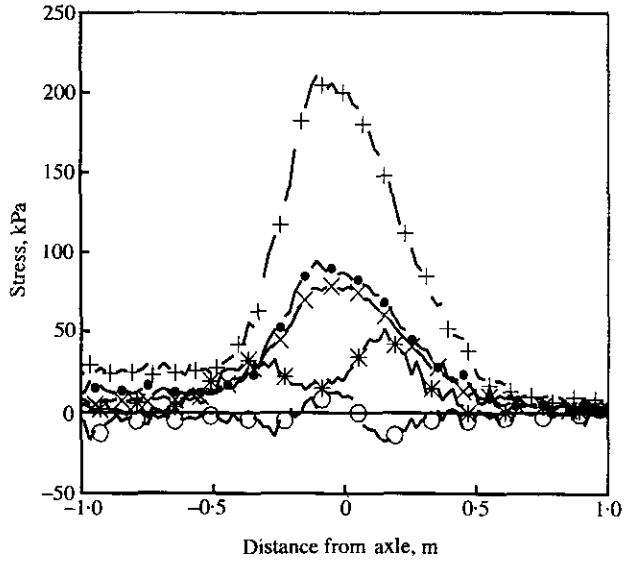

Fig. 6. Typical stresses beneath a tyre calculated from measurements made with a SST. σ_1(+), σ_2(*), σ_3(o) are principal stresses, σ_{oct}(×) is the octahedral normal stress and τ_{oct}(·) is octahedral shear stress

5.1. *The Frölich-modified Cerruti equation*

Johnson and Burt[18] used the Frölich and Cerruti equations to incorporate the soil–tyre interface stresses into a stress state prediction equation. The Frölich equation,[19] a version of the Boussinesq equation, predicts the radial normal stress in a semi-infinite, homogeneous, elastic half-space. Two basic assumptions of the Frölich equation are that the modulus of elasticity increases with depth and that Poisson's ration is 0·5. A Poisson's ratio of 0·5 indicates no volume change for an elastic material.[19] The Frölich equation can predict the radial normal stress, σ_r, at a point in the soil medium from a single normal point load on the surface. The Cerruti equation predicts the radial normal stress in the elastic half-space due to a single shear point load on the soil surface.[19] Johnson and Burt[18] modified the Cerruti equation to account for an increasing modulus of elasticity with depth and, using the principle of superposition, developed Eqn (8) to calculate σ_{r_i} for each point load applied at the soil surface

$$\sigma_{r_i} = \frac{n(P_i \cos^{n-2}\phi_i + H_i \sin^{n-2}\phi_i \cos\theta_i)}{2\pi R_i^2} \tag{8}$$

where n is the Frölich's concentration factor ($\geq 3{\cdot}0$); P_i is the normal point load; H_i is the shear point load; R_i is the radial distance from point load to desired point; ϕ is the angle between the normal load vector and the position vector from the point load to the desired point; and θ is the angle between the shear load vector and the vertical plane that contains the position vector from the shear load to the desired point. *Fig. 7* shows these geometric relationships. After the radial stresses

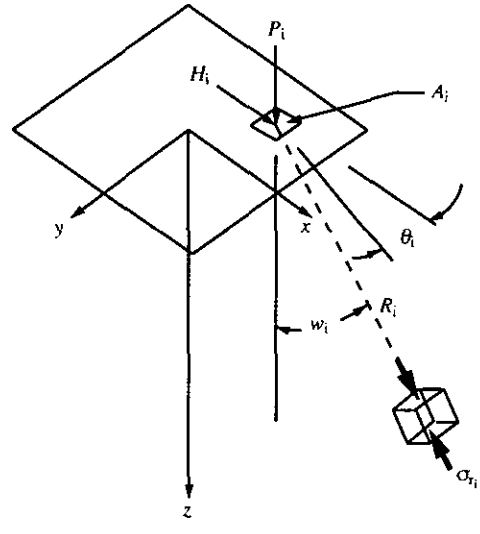

Fig. 7. Geometric relationships for the Frölich and modified Cerruti equations

are rotated into fixed orthogonal coordinates, they can be summed to determine the total stress tensor. The Frölich-modified Cerruti equation [Eqn (8)] was used to analyse the predicted stress states of different tyre footprints. However, since the Frölich and Cerruti equations were developed with the assumption of a Poisson's ratio of 0·5 (no volume change), it would not be valid to calculate volume changes from these stresses.

5.2. *Soil compaction prediction procedures by finite element analysis*

Stress and strain distribution within the soil profile can also be analysed using finite element analysis. The finite element method offers a great deal of flexibility, particularly with boundary conditions, and can handle complex situations such as different soil structures, hard pans and obstructions. Complex loading structures such as agricultural tyres and tillage implements can also be modelled accurately. The main limitations are individidual creativity and patience when setting up boundary conditions, and the amount of computational time available.

Existing finite element methods are based on the linear-elastic parameters, Young's modulus (E) and Poisson's ratio (ν), which define the relationships among stress, strain, and deformation. The stress–strain relationship for a linear-elastic material can be stated as:

$$\{\sigma\} = [C]\{\epsilon\} \tag{9}$$

where $\{\sigma\}$ is the stress vector; $\{\varepsilon\}$ is the strain vector; and $[C]$ is the constitutive matrix, a function of E and ν. Eqn (9) is the constitutive equation used in the finite element analysis of linear elastic materials such as many metals.

Agricultural soils, however, are not as well behaved as most metals. First, agricultural soils are susceptible to large strains and considerable compaction when they are moist and very loose. When soils are in this state, Young's modulus and Poisson's ratio must be determined from a compression test. This is usually accomplished using a triaxial apparatus with a confining cell pressure to prevent collapse of the soil sample. This confining pressure results in a normal stress perpendicular to the lateral directions, a condition different from the situation for metals. In fact, the results of a stress–strain test on soil are dependent on the confining pressure, σ_3, used during the test. Second, the results of this test on soil are highly non-linear and cannot be represented by single values of E and ν.

The most common technique used to handle the non-linearity of soil within a finite element analysis is an incremental approach. Instead of applying the entire load and determining the resulting deformations, stresses, and strains, the load is applied in incremental steps. The full load is divided into several smaller loads and an analysis is made for each of the load steps. The results are then accumulated until the full load has been applied. A tangential Young's modulus is calculated at each successive load step for the next progressive step. Poisson's ratio generally is considered constant.[20,21]

Perumpral *et al.*,[22] using an alternate definition for Young's modulus, calculated Young's modulus by examining a unique relationship between octahedral stress ratios and shear strain. Values of Young's modulus for successive steps were obtained from this relationship based on the loads of the current step. A single value of Poisson's ratio was assumed. Another common approach[23,24] is to use a hyperbolic stress–strain relationship to determine a tangential Young's modulus

$$E_t = \left[1 - \frac{R_f(1 - \sin\phi)(\sigma_1 - \sigma_3)}{2C\cos\phi + 2\sigma_3 \sin\phi}\right]^2 K p_a \left(\frac{\sigma_3}{p_a}\right)^n \tag{10}$$

where R_f is the failure ratio; C and ϕ are the Mohr-Coulomb failure envelope parameters; K is a modulus number; n is the exponent determining the rate of variation of the initial E with σ_3; p_a is atmospheric pressure; and σ_1, σ_3 are principal stresses. This approach has parameters that are easily determined from standard triaxial tests.

Duncan and Chang[25] recognized that Poisson's ratio should not be considered a constant under a general system of changing stresses. They calculated values of Poisson's ratio from triaxial tests using Eqn (11)

$$\nu = \frac{\Delta\epsilon_1 - \Delta\epsilon_v}{2\,\Delta\epsilon_1} \tag{11}$$

where $\Delta\epsilon_v$ is the incremental volumetric strain and $\Delta\epsilon_1$ is the incremental axial strain. They found that Poisson's ratio varied from 0·11 to 0·65 as deviatoric stress increased. However, Duncan and Chang did not use this equation in their finite element program because of computational difficulties.

Raper and Erbach[26] also questioned the role of Poisson's ratio during the soil compaction process. They used finite element analysis to analyse soil compaction under a flat plate. They reported that soil stress values were more dependent upon Poisson's ratio than on Young's modulus. Their results indicated the importance of both parameters throughout the

entire simulation cycle. If a high constant value of Poisson's ratio is assumed for initially loose soil, too much force will be transferred laterally. This will create excessive soil strength and restrict soil compaction during successive steps.

Raper and Erbach[27] used Eqn (11) to determine values of Poisson's ratio and the first derivative of Eqn (3) to determine values of Young's modulus in a finite element program designed to predict soil stresses and soil compaction. Stresses predicted by the finite element program were compared with stresses measured in a laboratory experiment. SSTs were buried in the soil and a flat circular steel plate was used to apply vertical loads to the soil surface. Values of octahedral normal stress calculated from the SST data compared favourably with predicted values from the finite element program (*Fig. 8*). Most of the stresses predicted by the finite element program were contained within the 95% confidence intervals of the SST stresses.

Raper *et al.*[28] further expanded their program to use the deviatoric stress model, Eqn (6), to predict soil stresses and compaction. These new predicted stresses were compared with the stresses from the circular flat plate experiment. Predicted values of octahedral normal stresses from the finite element program were generally greater than the stresses from the circular flat plate experiment. Only about 50% of the stresses predicted by the finite element program were contained within the 95% confidence intervals of the SST stresses.

The inaccuracies of soil stress predictions are currently being attributed to poor predictions of Poisson's ratio. Laboratory data from past research that were being used to relate the volumetric strain to axial strain were being extrapolated beyond their original range of stress ratios (Grisso *et al.*[29]). New developments in the constitutive relationship (Johnson and Bailey[30]) should enhance the finite element analysis and allow more accurate estimations of Poisson's ratio.

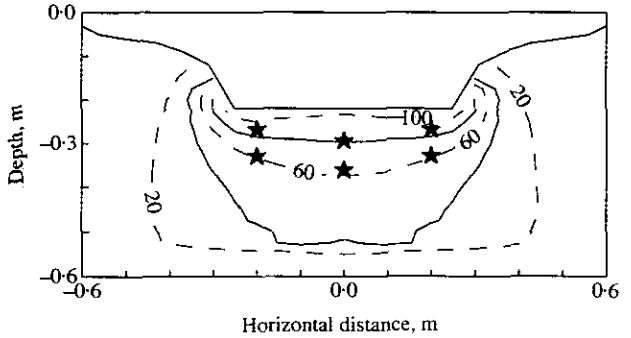

Fig. 8. Octahedral normal stress contours (kPa) under a load of 25 kN applied by a flat disc. Predicted by the finite element method. A hard pan was assumed to be located at a depth of 540 mm, and the stars indicate the positions of the SSTs

6. Conclusions

The results of research in several related areas are being integrated into a procedure to predict soil compaction from machinery traffic. Soil–tyre interface and soil profile stresses are being measured. Analytical and finite element analyses provide methods of presenting the stress distribution throughout the soil profile. Constitutive stress–strain relationships involving shear and normal stresses link the stresses in the profile to the resulting soil compaction and strain. The versatility and accuracy of the finite element analysis should increase with (i) continued improvements and refinements in constitutive equations for soils, (ii) further developments in techniques for handling nonlinear stress-strain behaviour, and (iii) integration of soil–tyre interface stresses into the finite element program. Simpler techniques of determining the soil parameters in the constitutive equations are also needed.

References

[1] **Schafer R L; Bailey A C; Johnson C E; Raper R L** A rationale for modeling soil compaction behavior: an engineering mechanics approach. Transactions of the ASAE 1991, **34**(4): 1609–1617

[2] **Vanden Berg G E; Gill W R** Pressure distribution between a smooth tire and the soil. Transactions of the ASAE 1962, **5**: 126–129, 132

[3] **Trabbic G W; Lask K V; Buchele W F** Measurements of soil-tire interface pressures. Agricultural Engineering 1959, **40**(1): 678–681

[4] **Krick G** Correlations between rigid wheel, pneumatic tire, and yielding soil. Dissertation, Doktor-Ingenieurs, Fakultat fuer Machinenwessen und Elektrotechnik der Technischen Universitat Muchen. Translation from German, 1958

[5] **Burt E C; Wood R K; Bailey A C** A three-dimensional system for measuring tire deformation and contact stresses. Transactions of the ASAE 1987, **30**(2): 324–327

[6] **Wood R K; Burt E C** Thrust and motion resistance from soil-tire interface stress measurements. Transactions of the ASAE 1987, **30**(5): 1288–1292

[7] **Wood R K; Burt E C; Johnson C E** Dynamic load effects on thrust components along the soil-tire contact zone. Transactions of the ASAE 1991, **34**(1): 43–46

[8] **Burt E C; Wood R K; Bailey A C** Some comparisons of average to peak soil-tire contact pressures. Transactions of the ASAE 1992, **35**(2): 401–404

[9] **Malvern L E** Introduction to the mechanics of a continuous medium. Prentice-Hall, Inc. Englewoods Cliffs, N.J. 1969

[10] **Vanden Berg G E; Buchele W F; Malvern L E** Application of continuum mechanics to soil compaction. Transactions of the ASAE 1958, **1:** 24–27

[11] **Söhne W; Chancellor W J; Schmidt R H** Soil deformation and compaction during piston sinkage. Transactions of the ASAE 1962, **5:** 235–239

[12] **Bailey A C; Vanden Berg G E** Yielding by compaction and shear in unsaturated soils. Transactions of the ASAE 1968, **11**(3): 307–311, 317

[13] **Roscoe K H; Schofield A N; Worth C P** On the yielding of soils. Geotechnique 1958, **9**(8): 71–83

[14] **Bailey A C; Johnson C E; Schafer R L** A model for agricultural soil compaction. Journal of Agricultural Engineering Research 1986, **33:** 257–262

[15] **Bailey A C; Johnson C E** A soil compaction model for cylindrical stress states. Transactions of the ASAE 1989, **32**(3): 822–825

[16] **Nichols T A; Bailey A C; Johnson C E; Grisso R D** A stress state transducer for soil. Transactions of the ASAE 1987, **30**(5): 1237–1241

[17] **Harris W L** 1960. Dynamic stress transducers and the use of continuum mechanics in the study of various soil stress–strain relationships. Unpublished Ph.D. dissertation. Michigan State University, East Lansing, MI

[18] **Johnson C E; Burt E C** A method of predicting soil stress state under tires. Transactions of the ASAE 1990, **33**(3): 713–717

[19] **Feda J** Stress in subsoil and methods of final settlement calculation. New York: Elsevier Scientific Publishing Co., 1978

[20] **Raper R L; Gassman P W; Erbach D C; Melvin S W** Agricultural soil modeling using finite-element analysis. ANSYS Conference Proceedings, Newport Beach, CA, 1987

[21] **Chi L; Kushwaha R L** A non-linear 3-D finite element analysis of soil failure with tillage tools. Journal of Terramechanics 1991, **27**(4): 343–366

[22] **Perumpral J V; Liljedahl J B; Perloff W H** The finite element method for predicting stress distribution and soil compaction under tractive devices. Transactions of the ASAE 1971, **14**(6): 1184–1188

[23] **Pollock D Jr; Perumpral J V; Kuppusamy T** Finite element analysis of multipass effects of vehicles on soil compaction. Transactions of the ASAE 1985, **29**(1): 45–50

[24] **Chi L; Kushwaha R L** A non-linear 3-D finite element analysis of soil failure with tillage tools. Journal of Terramechanics 1991, **27**(4): 343–366

[25] **Duncan J M; Chang C Y** Nonlinear analysis of stress and strain in soils. Journal of the Soil Mechanics and Foundations Division. American Society of Civil Engineers 1970, **96**(5): 1629–1653

[26] **Raper R L; Erbach D C** Effect of variable linear elastic parameters on finite element prediction of soil compaction. Transactions of the ASAE 1990, **33**(3): 731–736

[27] **Raper R L; Erbach D C** Prediction of soil stresses using finite element analysis. Transactions of the ASAE 1990, **33**(3): 725–730

[28] **Raper R L; Johnson C E; Bailey A C** Coupling normal and shearing stresses to use in finite element analysis of soil compaction. Transactions of the ASAE 1994, **37**(5): 1417–1422

[29] **Grisso R D; Johnson C E; Bailey A C** The influence of stress path on distortion during soil compaction. Transactions of the ASAE 1987, **30**(5): 1302–1307

[30] **Johnson C E; Bailey A C** A shearing strain model for cylindrical stress states. American Society of Agricultural Engineers, Paper 90-1085, 1990